Int. J. Hyperthermia, December 2010; 26(8): 748–764

informa
healthcare

RESEARCH ARTICLE

Measurement and mathematical modeling of thermally induced injury and heat shock protein expression kinetics in normal and cancerous prostate cells

MARISSA NICHOLE RYLANDER[1], YUSHENG FENG[2], KRISTEN ZIMMERMANN[3], & KENNETH R. DILLER[4]

[1]*School of Biomedical Engineering and Sciences and Department of Mechanical Engineering, Virginia Tech, Blacksburg, Virginia,* [2]*Department of Mechanical Engineering, University of Texas at San Antonio, Texas,* [3]*School of Biomedical Engineering and Sciences, Virginia Tech, Blacksburg, Virginia, and* [4]*Department of Biomedical Engineering, Institute for Cellular and Molecular Biology, University of Texas at Austin, Texas, USA*

(Received 24 January 2010; Revised 26 March 2010; Accepted 15 April 2010)

Abstract

Purpose: Hyperthermia can induce heat shock protein (HSP) expression in tumours, which will cause enhanced tumour viability and increased resistance to additional thermal, chemotherapy, and radiation treatments. The study objective was to determine the relationship of hyperthermia protocols with HSP expression kinetics and cell death and develop corresponding computational predictive models of normal and cancerous prostate cell response.

Methods: HSP expression kinetics and cell viability were measured in PC3 prostate cancer and RWPE-1 normal prostate cells subjected to hyperthermia protocols of 44° to 60°C for 1 to 30 min. Hsp27, Hsp60, and Hsp70 expression kinetics were determined by western blotting and visualised with immunofluorescence and confocal microscopy. Based on measured HSP expression data, a mathematical model was developed for predicting thermally induced HSP expression. Cell viability was measured with propidium iodide staining and flow cytometry to quantify the injury parameters necessary for predicting cell death following hyperthermia.

Results: Significant Hsp27 and Hsp70 levels were induced in both cell types with maximum HSP expression occurring at 16 h post-heating, and diminishing substantially after 72 h. PC3 cells were slightly more sensitive to thermal stress than RWPE-1 cells. Arrhenius analysis of injury data suggested a transition between injury mechanisms at 54°C. HSP expression and injury models were effective at predicting cellular response to hyperthermia.

Conclusion: Measurement of thermally induced HSP expression kinetics and cell viability associated with hyperthermia enabled development of thermal dosimetry guidelines and predictive models for HSP expression and cell injury as a function of thermal stress to investigate and design more effective hyperthermia therapies.

Keywords: *Hsp27, Hsp60, Hsp70 expression kinetics, HSP expression model, cell viability, cell injury model, prostate cancer*

Introduction

Prostate cancer is the second leading cause of cancer-related deaths for males in the United States, exceeded only by lung cancer, with one in six men expected to contract the disease during their lifetime [1]. Radical prostatectomy or radiation therapy are primary treatments for prostate cancer. However, both modalities are associated with urinary and or bowel morbidity and erectile dysfunction. Minimally invasive energy-based treatments, such as thermal ablation [2, 3], local hyperthermia with or without the aid of magnetic nanoparticles [4, 5], hyperthermia sensitisation for use in conjunction with radiotherapy [6, 7], chemotherapy [8, 9], brachytherapy [10, 11], and thermally mediated drug or gene therapy deliveries [12–14], may provide superior alternatives to radical prostatectomy or radiation therapy. The ability to enable a reasonable

Correspondence: Marissa Nichole Rylander, Assistant Professor, School of Biomedical Engineering and Sciences and Department of Mechanical Engineering, Virginia Tech, ICTAS Building, Stanger Street, Blacksburg, VA 24060, USA. Tel: (540) 231-3134. E-mail: mnr@vt.edu

ISSN 0265–6736 print/ISSN 1464–5157 online
DOI: 10.3109/02656736.2010.486778

prediction of the outcome at the time of treatment delivery is critical to the success of each of these therapies.

Predictions of thermal necrosis in regions where injury is severe can be achieved with knowledge of the temperature history versus time during treatment. However, in regions where temperatures are insufficient to coagulate proteins, the results and subsequent impact on therapy outcomes are difficult to determine [15]. Applied thermal stress is often considered a mediator for hyperthermic cell necrosis; conversely, it also elicits an up-regulation of heat shock proteins (HSPs) to protect cancer cells. [16–20]. Thermally induced HSP expression can enhance tumour cell viability and impart resistance to chemotherapy and radiation when hyperthermia is applied prior to these procedures [20–23]. Consequently, knowledge of the thermal dose necessary to induce or de-activate HSP expression in the prostate is essential for designing an effective thermal therapy for hyperthermia alone or as an adjuvant to radiotherapy or chemotherapy.

Molecular chaperons such as HSPs have been implicated in many roles of therapeutic resistance including multi-drug resistance [24–26], regulation of apoptosis [27–31], and modulation of p53 functions [28, 32, 33] for a broad range of neoplastic tissues. The present study focuses on characterising the thermally induced kinetics of three dominant HSPs associated with prostate cancer progression: Hsp27, Hsp60, and Hsp70. Hsp27 is normally expressed at low levels under non-stress conditions within the cytosol of human cells. In prostate cancers, over-expression of Hsp27 is a poor prognostic marker for invasive prostatic carcinoma, but the absence of Hsp27 is a reliable objective marker in early prostatic neoplasia [22]. Elevated Hsp27 levels have been associated with tumour cell protection by inhibition of apoptosis [28, 33]. It has also been suggested that Hsp27 and Hsp70 modulates reactive oxygen species by means of a glutathione-dependent pathway [34, 35], providing protection for intracellular proteins and partially explaining their protective effect against chemotherapeutic agents [23, 33, 36, 37].

Hsp60 is in abundance within the majority of mammalian cells under normal conditions [38], where it functions primarily in chaperoning and folding proteins [39]. Both Hsp60 and Hsp70 have been identified for their roles in antigen processing, presentation, and transportation of the tumour rejection antigens on the membrane of tumour cells [39, 40]. Thus, they enable cancer-specific immunity due to chaperoning antigenic peptides [40–43]. Enhanced expression of Hsp60 has been observed in breast carcinoma [38], myeloid leukaemia [44], and early and advanced cases of prostate cancer [22].

Increased expression of Hsp70 protects proteins from the damaging effects of stress [45, 46]. This has been observed in several types of tumours, including breast and cervical cancers [33, 47], and its mechanism may be involved in cell proliferation, prognosis, and drug resistance [26, 48, 49]. A study performed by Beckham et al. illustrated that Hsp70 is necessary for cell survival by comparing Hsp70 knockout murine embryonic fibroblasts (MEF) and control MEF cellular responses to various mild heat treatments [46]. Recent evidence suggests Hsp70 has a role in the control of cell cycling and growth [37, 50, 51]. A positive correlation between Hsp70 levels and proliferative activity has been demonstrated in immunohistochemical studies of breast tumours [21].

Cellular studies have demonstrated the effectiveness of thermal stress in enhancing HSP expression and confirmed greater cellular resistance to injury during subsequent exposure to radiation or chemotherapeutic agents. Human androgen-dependent (LNCaP) and androgen-independent cells (PC3) demonstrated increased expression of Hsp27 and Hsp70 and significantly reduced chemical- and radiation-induced apoptosis following incubator heating at 42°C for 0, 60, and 120 min [28]. *In vivo* studies in which prostate tumours were treated with trans-rectal high-intensity focused ultrasound (HIFU) exhibited an intra-prostatic thermal necrosis zone with the maximum temperature elevation of 100°C and a peripheral zone at the tumour border characterised by sub-lethal temperatures (45–50°C), massive up-regulation of Hsp27 expression, and high cell viability [16]. Other studies have utilised a bioluminescent reporter gene to measure Hsp70 expression, determine the zone of thermal damage [52], and provide more comprehensive characterisation of cell death kinetics after heat shock [46, 53]. This technique can be adapted to in vivo models which is imperative in determining effective thermal therapy protocols [54].

Although previous studies have documented increased HSP expression in prostate cells following hyperthermia, no characterisation of the thermally induced HSP kinetics exists, which is essential for dosimetry guideline development for prostate cancer therapy [17]. Furthermore, no mathematical models can predict HSP expression kinetics in response to hyperthermia. Rieger et al. developed a mathematical model for describing the critical steps in the regulation of heat-shock transcription factor-1 (HSF1) activity which directly results in the elevated expression of genes encoding molecular chaperones [55]. However, this model is not capable of predicting HSP expression dynamically in response to thermal stress. A more comprehensive characterisation of thermally induced cell death kinetics for

normal and cancerous prostate cells and subsequent determination of Arrhenius injury parameters are also needed critical components for predicting and controlling the extent of tumour and healthy tissue destruction associated with hyperthermia therapies. Finally, the correlation between HSP expression and cellular injury is required to accurately predict tumour cell response.

This study was designed to measure thermally induced Hsp27, Hsp60, and Hsp70 expression and cell injury kinetics. The correlation between cell viability and HSP expression in prostate cancer (PC3) cells and normal (RWPE-1) cells for temperatures and exposure durations typically encountered in hyperthermia therapy was also investigated. Visualisation of HSP expression in PC3 and RWPE-1 cells following thermal stress was performed to understand the localisation of specific HSPs within the cell. The HSP kinetics data was employed to develop a mathematical predictive model for HSP expression based on a prescribed thermal stress to control HSP expression and optimise thermal therapies. Determination of Arrhenius injury parameters based on cell viability kinetics data enabled the prediction of cellular injury for a wider range of heating protocols. A correlation between thermally induced alterations in cell viability and HSP expression was determined to enable a more accurate prediction of the prostate cell's response to hyperthermia. This data should support the investigation of advanced hyperthermia protocols. For example, a protocol that minimises HSP expression in the tumour region and elevates expression in the healthy surrounding tissue to produce maximum tumour destruction and preservation of healthy tissue, respectively, may be beneficial.

Materials and methods

Cell culture

PC3 cells (CRL-1435, ATCC, Manassas, VA) were cultured with HAM's F12 medium (30-2004, ATCC) with 10% fetal bovine serum (30-2020, ATCC) and 5% penicillin-streptomycin (15140-122, Gibco, Carlsbad, CA). RWPE-1 cells (CRL-11609, ATCC) were cultured with keratinocyte serum free medium (BRL 17005-042, Gibco) supplemented with $5\,ng\,mL^{-1}$ human recombinant epidermal growth factor and $0.05\,mg\,mL^{-1}$ bovine pituitary extract. Cultures were maintained in a 5% CO_2 incubator in $250\,mm^2$ phenolic culture flasks to prevent contamination from leakage during the heating process.

Hyperthermia protocol

A constant temperature circulating water bath (NESLAB RTE-100, Thermo Electron Corporation, San Jose, CA) was employed as the hyperthermia source to produce a relatively short thermal time constant of 4 seconds to heat experimental specimens as calibrated in prior work [17]. The water bath, temperature monitoring devices, and all other accessories remained in a sterile hood throughout the experiment to prevent contamination of the cells. Sterilised medium containing Eagle's Minimum Essential Medium (MEM) without L-glutamite was added to a polyethylene bottle and placed in the same bath used for cell heating. A sterilised thermal probe was inserted into the bottle to monitor media temperature and a thermocouple measured water bath temperature. Water within the bath and the heating medium were warmed until they equilibrated to within 0.1°C of the target temperature. Upon reaching confluence, cells were rinsed with phosphate buffered saline (PBS) to prevent cell damage caused by the degradation of L-glutamite at high temperatures. The flask was filled with 70 mL of heating medium with the bottle held in the bath and the flask was submerged in the water bath for a predetermined temperature and duration in the ranges of 44–60°C for 1–30 min. The maximum experimental temperature caused complete cell death for the shortest heating duration. Following heating, cells were rinsed with PBS and the flasks were returned to a 37°C incubator for subsequent manifestation of injury and HSP expression.

Hsp27, Hsp60, and Hsp70 expression evaluation

After an incubation time of 16 h post-heating (shown to be an effective evaluation period for measuring Hsp70 expression in previous work [17, 56]), cells were lysed in buffer solution (5M NaCl, 1% IGEPAL, 0.5% sodium deoxycholate, and 10% sodium dodecyl sulfate were dissolved in 100 mL H_2O). Protease inhibitors consisting of leupeptin ($10\,mg\,mL^{-1}$ in H_2O), pepstatin ($1\,mg\,mL^{-1}$ in methanol), aprotinin ($10\,mg\,mL^{-1}$ in PBS), and phenylmethylsulphonylfluoride (PMSF) ($10\,mg\,mL^{-1}$ in isopropanol) were also added to the lysis buffer to preserve protein integrity. HSP expression in the PC3 cells was also measured for post-heating durations of 24, 48, and 72 h. The total protein concentration for each sample was evaluated using a spectrophotometer (DU 530, Beckman, Irvine, CA) at 595 nm and a protein dye assay (500-0002, Bio-Rad Labs, Hercules, CA) to permit determination of correct volume for loading of equal protein concentrations in gels. All wells of Criterion Pre-cast Gels (345-0009, Bio-Rad Labs) for gel-electrophoresis were loaded with 20 μg of protein with varying volumes to permit equal amounts of

protein loaded for each sample. The separated proteins were transferred to polyvinylidene difluoride (PVDF) membranes (162-0175, Bio-Rad Labs) by immunoblot. Membranes underwent blocking in 3% non-fat dry milk blotto for 1.5 h at room temperature (RT) to remove non-specific proteins. Subsequently, primary antibodies were diluted in 3% non-fat dry milk blotto according to the following: anti-Hsp27 IgG1 mouse monoclonal (SPA-800, Stressgen Biotechnologies, San Diego, CA) at a dilution of 1:1000, anti-Hsp60 IgG1 mouse monoclonal (SPA-806, Stressgen) at a dilution of 1:40,000, anti-Hsp70 IgG1 mouse monoclonal (SPA-810, Stressgen) at a dilution of 1:1000, and anti-actin goat IgG (sc-1616, Santa Cruz Biotechnology, CA) at a dilution of 1:2000. Membranes were incubated with primary antibodies for 1.5 h at RT. Next, membranes were incubated with secondary antibodies: donkey anti-goat IgG-HRP (sc-2020, Santa Cruz Biotechnology) at a dilution of 1:10,000 and goat anti-mouse IgG1-HRP (sc-2969, Santa Cruz Biotechnology) at a dilution of 1:3000 both in 3% non-fat dry milk blotto for 1 h at RT. Monoclonal antibodies were employed to increase specificity for the three HSPs and to decrease background effects. A polyclonal antibody was used for actin because it produced a stronger signal than its monoclonal counterpart. Protein bands were visualised by incubating with a chromogenic substrate tetramethylbenzidine (TMB) (SK-4400, Vector Laboratories, Burlingame, CA) and the protein bands were analysed quantitatively with Image Pro Plus (Media Cybernetics, San Diego, CA) in terms of size and mean density. The amount of protein for each sample was represented as the area under the intensity histogram of the corresponding band. Protein concentration was calculated as the product of the band area and mean density. The ratios of Hsp27, Hsp60, and Hsp70 were normalised to actin concentration to account for possible variations in total protein measured for each sample and for different background effects among membranes.

Hsp27, Hsp60, and Hsp70 expression visualisation

Immunofluorescence permitted imaging of the Hsp27 and Hsp70 distributions within the PC3 cells following heating using previously published methods [57, 58]. After heating, cells were fixed with methanol and permeabilised with 0.1% Triton X-100 in PBS for 5 min in an incubator ($T = 37^{\circ}$C and 5% CO_2). Cells then underwent blocking in 1.5% goat anti-mouse serum (sc-2043, Santa Cruz Biotechnology) for 1 h. Next, cells were incubated with the Hsp70 primary mouse monoclonal IgG_{2A} antibody (sc-24, Santa Cruz Biotechnology) at a 1:50 dilution in 1.5% goat anti-mouse serum for 1 h followed by incubation with its secondary antibody Rhodamine Red-X (IgG_{2A}) (115-295-206, Jackson ImmunoResearch, West Grove, PA) for a 1:50 dilution in PBS. Cells were then incubated with biotinylated Hsp27 mouse monoclonal IgG_1 primary antibody (SPA-800B, Stressgen) for a 1:150 dilution in PBS followed by incubation with its secondary antibody, Cy2 conjugated streptavidin antibody, (016-220-084, Jackson ImmunoResearch) for a 1:300 dilution in PBS. Observation of HSP expression levels were accomplished with a 3D laser scanning confocal microscopy with a magnification of 60X. An argon laser ($\lambda = 488$ nm) was employed for excitation of the Cy2 conjugated streptavidin antibody to enable visualisation of Hsp27 expression. A HeNe laser ($\lambda = 543$ nm) was utilised for excitation of the Rhodamine Red-X dye for visualisation of Hsp70 expression.

HSP expression model

The measured thermally induced HSP expression data from western blotting enabled determination of the HSP expression kinetics associated with a thermal stimulus. The objective was to determine a mathematical formulation to represent the measured in vitro data and yield insight into the thermally induced HSP expression kinetics for a more extensive set of conditions than were experimentally measured. Elevated HSP expression is initiated by the presence of denatured proteins caused by exposure to thermal stress for extended time [17–21]. HSP expression induction is dependent on the temperature elevation, duration of stimulus exposure, and other biological factors [59, 60]. A model was developed that describes HSP expression as a function of temperature, T, and heating duration, t, normalised with respect to actin concentration and defined as $H(t,T)$ based on our experimental data [61, 62]. Non-stressed cells possessed a characteristic basal level of HSP expression that was unique for both RWPE-1 and PC3 cells. HSP expression was normalised with respect to the basal level so that at $t = 0, H(t, T)|_{t=0} = 1$. Following heat shock, HSP expression rose with increasing time initially and accumulation of denatured proteins was observed. Eventually, HSP expression dramatically declined as the injury to the cell became so substantial that the cell machinery could no longer synthesise additional HSPs and the existing basal level of HSP was denatured. To capture this phenomena, the mathematical form of $H(t, T)$ must satisfy $\lim_{t\to\infty} H(t, T) = 0$, i.e., $H(t, T)$ needs to eventually vanish for extensive heating durations due to extreme injury and protein denaturation, as shown in the results section, in Figures 3 and 4. This phenomenon occurred at each measured

temperature; but with increasing temperatures, the peak HSP expression and its subsequent decline occurred earlier. Based on the measured HSP expression data, it is evident that a more complicated kinetic phenomenon transpires which cannot be described by a first order chemical reaction, such as the reaction embodied in the Arrhenius injury equation described subsequently. It is postulated that the rate of change of HSP expression based on a transient thermal stress is proportional to the HSP expression concentration itself according to a non-linear proportional rate coefficient, C, dependent on both heating duration and temperature referred to as the function, $C(t, T)$. Thus, the general form of the rate of HSP expression can be viewed as:

$$\partial_t H(t, T) \alpha C(t, T) - H(t, T) \tag{1}$$

where $\partial_t(\cdot)$ denotes the partial derivative of $H(t,T)$. One form to satisfy Equation 1 and fit the HSP data accurately can be embodied in the following expression:

$$H(t, T) = Ae^{(\alpha(T)t - \beta(T)t^{\gamma(T)})} \tag{2}$$

where $\alpha(T)$, $\beta(T)$, and $\gamma(T)$ are HSP expression kinetics parameters that are independent of time, but are dependent on temperature. We further impose a restriction of $\gamma > 1$ and frequent use of $A = 1$ (due to normalisation of basal HSP expression at $t = 0$) [61, 62]. These parameters were determined using non-linear least square regression and are tabulated in Table I in the results section. The accuracy of this mathematical description for predicting HSP expression following laser irradiation of PC3 tumours has been confirmed previously by comparing model predicted and experimentally measured HSP expression using immunofluorescence staining and confocal microscopy [61].

Cell viability

Cell viability was assessed by propidium iodide (P3566, Molecular Probes, Carlsbad, CA) staining with a flow cytometer as previously described [63]. Following 72 h post-heating (shown to be an effective evaluation period for measuring the extent of cell death [17]), cells were trypsinised, pelleted, and resuspended in 4 mL PBS. Prior to the cell viability measurement, propidium iodide (1:1000 dilution in PBS) was added to the cell suspension and the percentage of dead cells was measured with a flow cytometer (Beckman, Irvine, CA) using an argon laser ($\lambda = 480$ nm). WinMDI 2.8 software allowed generation of histograms and analysis of data. Samples of unheated controls and cells necrosed by methanol treatment (70% methanol for 30 min) and extreme heat shock (60°C, 5 min) were used to calibrate regions of the histogram denoting live and dead cell populations. The region of the histogram occupied by the control (unheated) sample was defined as the live cell population with low levels of propidium iodide staining. The dead cell population was defined as the region of the histogram occupied by the methanol-treated and severely heat shocked sample, which also corresponded to the region excluding the control sample live population. The percentage of dead cells were converted to live cell values and normalised with the percentage of live cells for the control. The normalised percentage of live cells provided the value for C_τ characterised in the injury calculations. Cells were also counter-stained with calcein AM to confirm cell viability and provide comparison to the converted live cell values from propidium iodide staining.

Cell injury analysis

The availability of both thermal history and measured cell viability data enabled determination of parameter values for an Arrhenius injury model. This model permits prediction of cell injury for a wider range of heating protocols than experimentally measured [64]:

$$\Omega(\tau) = \ln\left(\frac{C_o}{C_\tau}\right) \tag{3}$$

$$\Omega(\tau) = A\int_0^\tau e^{-\frac{E_a}{\Re T(t)}}\,\mathrm{d}t \tag{4}$$

where cell injury, Ω, is defined as the logarithm of the ratio of the initial concentration of healthy cells, C_o, to the concentration of healthy cells remaining after thermal stimulation, C_τ, for a duration of $\tau(s)$. Important parameters are defined as frequency factor which is associated with the activation entropy, $A(s^{-1})$, activation energy of the thermal injury process, E_a ($\mathrm{J\,mol^{-1}}$), which is associated with activation enthalpy, universal gas constant, $\Re$ ($8.315\,\mathrm{J\,mol^{-1}\,K^{-1}}$), and instantaneous absolute temperature of the cells during stress, $T(K)$, which is a function of time, t (s). Equation 3 can be used to directly calculate cell injury from measured cell viability data and Equation 4 can enable prediction of injury data based on known E_a and A parameters.

Results

Determination of HSP expression

Western blotting. A western blot for PC3 and RWPE-1 cells heated at 44°C is shown in Figures 1A and 1B, respectively, demonstrating typical Hsp27, Hsp60, and Hsp70 expression levels for both cell types. Increasing heating duration

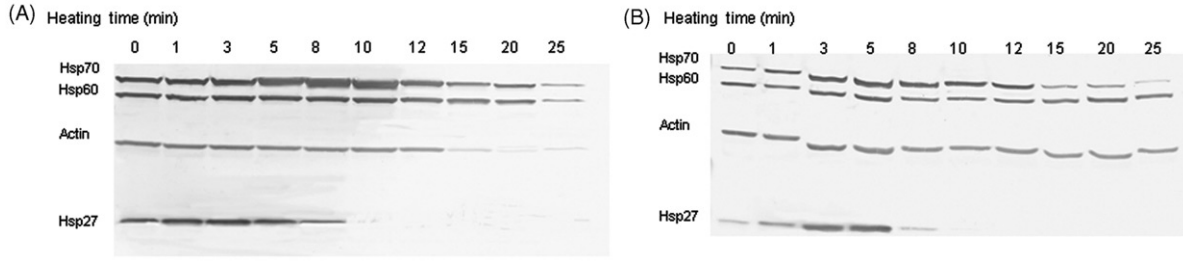

Figure 1. Western blots depicting Hsp27, Hsp60, and Hsp70 and actin levels for (A) PC3 and (B) RWPE-1 cells heated at 44°C for various heating durations, $n = 3$.

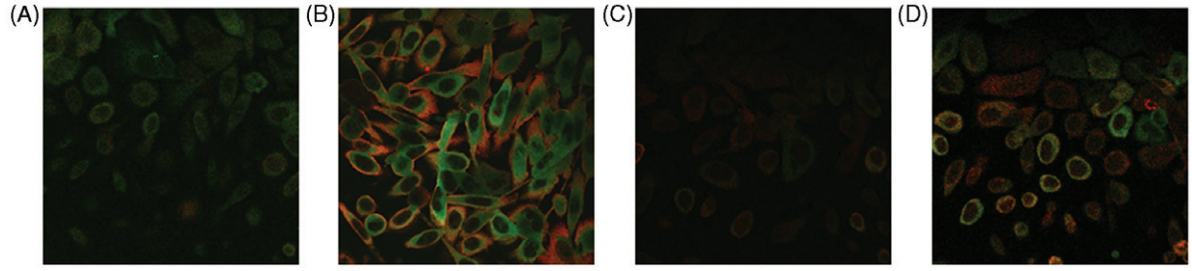

Figure 2. Distribution of Hsp27 (green fluorescence) and Hsp70 (red fluorescence) in PC3 cells (A) unheated (maintained at 37°C in incubator) and (B) heated ($T = 44$°C for 5 min) and RWPE-1 cells (C) unheated and (D) heated at $T = 44$°C for 5 min.

correlated with elevations in Hsp27 and Hsp70 expression as denoted by larger band size for longer heating durations for both cell types. The basal and thermally induced levels of Hsp27 and Hsp70 expression were higher for the PC3 cells. At extended heating durations (15 min for Hsp70 and 8 min for Hsp27) the thermal injury to PC3 and RWPE-1 cells was so extensive that the cell machinery could no longer produce HSP expression and the existing HSPs were also denatured, as denoted by the diminishing band size. This phenomenon was characteristic for both cell types at all temperatures. There was virtually no increase in Hsp60 expression due to the hyperthermia therapy.

Immunofluorescence

The Hsp27 (green fluorescence) and Hsp70 (red fluorescence) expression distributions for non-heated (maintained at 37°C in incubator) and heated (44°C for 5 min) PC3 (Figures 2A and 2B) and RWPE-1 cells (Figures 2C and 2D) were visualised using immunofluorescence and confocal microscopy. Higher basal and thermally induced levels of Hsp70 and Hsp27 expression were evident in the PC3 cells compared to expression in the RWPE-1 cells. Also the Hsp70 expression was concentrated in the periphery of the cytoplasm, whereas Hsp27 expression was observed in more interior regions of the cytoplasm for the PC3 cells. This distribution was characteristic of PC3 cells for all hyperthermia protocols considered. The localisation of Hsp27 and Hsp70 expression within the RWPE-1 cells appeared rather variable with Hsp70 expression accumulation in the periphery of some cells, while localising more extensively in the nucleus of other cells.

PC3 HSP kinetics

The normalised Hsp27, Hsp60, and Hsp70/actin expression kinetics data for PC3 cells measured by western blotting is shown in Figure 3 as a function of heating time following 16 h post heating (PH). The standard deviation values for measurement of HSP expression were not shown for clarity, but were in the range of 0.07–0.17 mg mL^{-1} with an average standard deviation of ± 0.12 mg mL^{-1}. Each HSP had a unique basal level of expression, as determined for the unheated control sample, but all HSP/actin values were normalised to ensure consistency of interpretation. Significant increases in Hsp27 and Hsp70 concentrations occurred following hyperthermia treatment, whereas Hsp60 elevation was minimal. The Hsp27 expression levels for all temperatures were more than twice that for Hsp70. The maximum expression levels for Hsp70 and Hsp27 occurred for the same hyperthermia protocol of 1 min at 50°C, with values of 2.7 and 8.8 times the control, respectively. The maximum Hsp60 expression occurred at 46°C for 25 min with a value 1.3 times the control. At lower temperatures, the rates

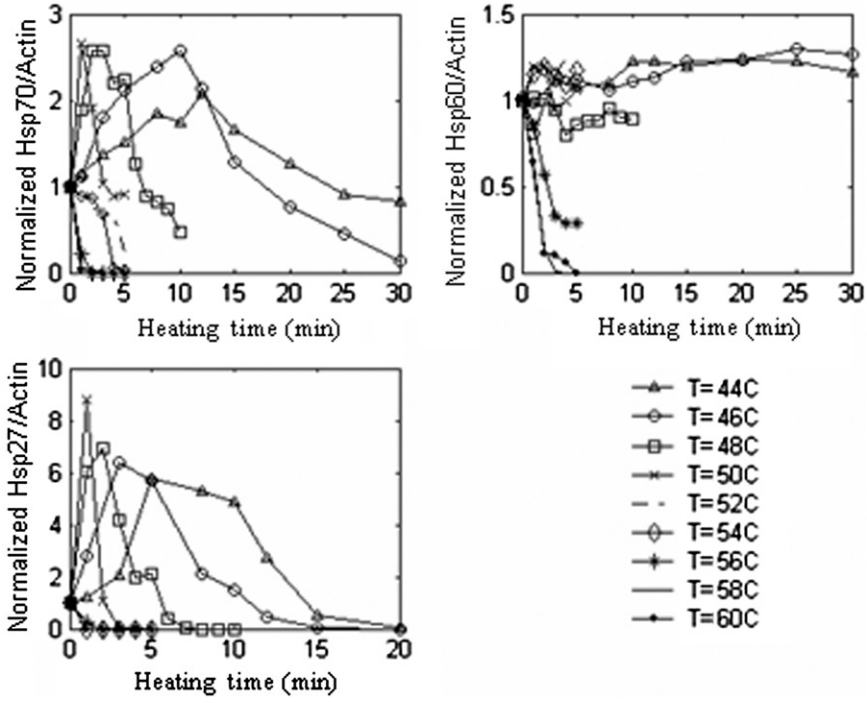

Figure 3. Normalised Hsp27/actin, Hsp60/actin, and Hsp70/actin expression ratios as a function of heating time and temperature determined with western blotting and evaluated at 16 h PH, $n = 3$ for PC3 cells with an average standard deviation in HSP expression measurement of $\pm 0.12\,\mathrm{mg\,mL^{-1}}$.

of all HSP expression decreased progressively. Temperatures greater than 50°C yielded minimal HSP expression and dramatic declines in cell viability.

RWPE-1 HSP expression kinetics

Normal prostate cells (RWPE-1) were exposed to the same hyperthermia protocols as the PC3 cells to determine whether there was a differential thermal stress response in these two cell types that could be manipulated advantageously for thermal therapy design. The normalised Hsp27, Hsp60, and Hsp70/actin expression kinetics data measured with western blotting are shown in Figure 4 for RWPE-1 cells. These cells were stressed for incremental heating temperatures and times and measured at 16 h PH. The Hsp27 and Hsp70 expression levels were much lower than were induced in PC3 cells. Maximum expression levels of 3.8, 1.5, and 2.3 times the control occurred for Hsp27, Hsp60, and Hsp70, respectively, for thermal stress at 50°C for 3 min in all three cases. The standard deviation values for HSP expression measurement were not shown for clarity and ranged from 0.08–0.21 $\mathrm{mg\,mL^{-1}}$ with an average standard deviation of $\pm 0.15\,\mathrm{mg\,mL^{-1}}$.

Time course of HSP expression

Although the period of stress requisite to elicit HSP over-expression may be relatively short (measured in minutes), the resultant HSP elevation in the affected tissue may last up to several orders of magnitude longer in time. This extended period can have important consequences for clinical treatment protocols, such as subsequent thermal, chemotherapy, or radiation treatments. Thus, the present experiments were designed to measure the duration of HSP expression elevation.

Hsp27, Hsp60, and Hsp70 concentrations were measured at various post-heating times (16, 24, 48, and 72 hours) following hyperthermia, as shown in Figure 5, to characterise the time course of expression in PC3 cells under hyperthermic conditions ($T = 44$°C for 1–30 min). The HSP value was normalised to 1, which was equivalent to the basal level of expression for each HSP. The highest measured expression typically occurred at 16–24 h PH, with peak normalised values for Hsp27, Hsp60, and Hsp70 of 5.8, 1.2, 2.1 times the control, respectively. For the majority of heating protocols, all HSP expression had decreased significantly by 48 h PH and was nearly absent at 72 h PH. The standard deviation values for HSP expression measurement were in the range of 0.05–0.18 $\mathrm{mg\,mL^{-1}}$ with an average standard deviation of $\pm 0.12\,\mathrm{mg\,mL^{-1}}$.

HSP expression predictive model

HSP expression model parameters were identified to fit the HSP expression predictive model to the Hsp27 and Hsp70 kinetics measured with western blotting

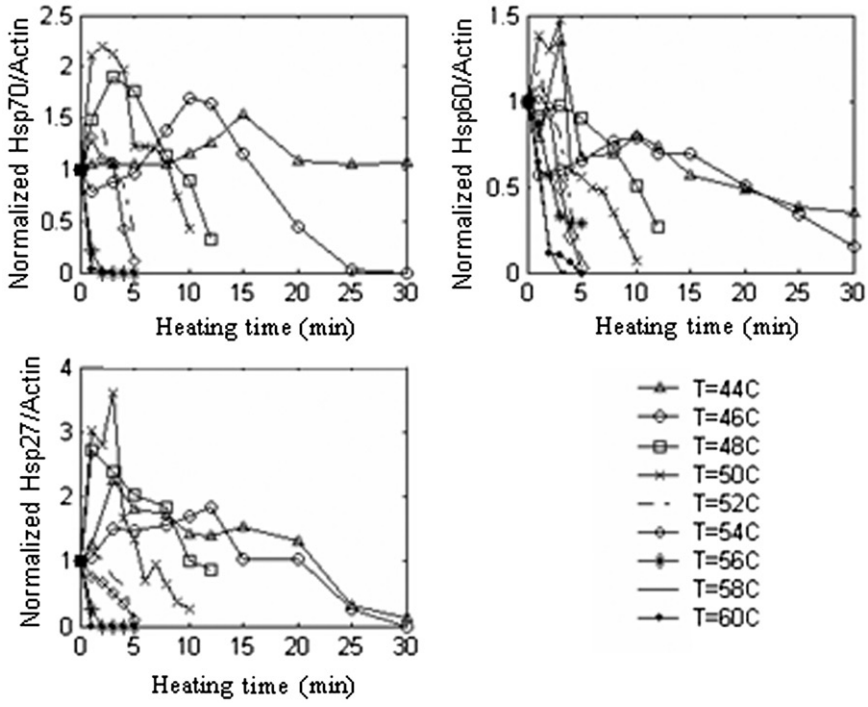

Figure 4. Normalised Hsp27/actin, Hsp60/actin, and Hsp70/actin expression ratios as a function of heating time and temperature determined with western blotting and evaluated at 16 h PH, $n = 3$ for RWPE-1 cells with an average standard deviation in HSP expression measurement of $\pm 0.14\,\mathrm{mg\,mL^{-1}}$.

for both PC3 and RWPE-1 cells. The model was not formulated for Hsp60 expression since there was minimal elevation in expression due to elevated temperatures. The determined Hsp27 and Hsp70 expression model parameter values for both cell types are shown in Table I. We observe that γ is nearly one, although the ranges of the other parameters vary. The model predicted and measured Hsp27 and Hsp70 kinetics for both PC3 and RWPE-1 cells were compared in Figure 6.

The correlation coefficients for the fit between the HSP expression curves generated for each temperature by the predictive model and the measured HSP kinetics curve were calculated for both Hsp27 and Hsp70 for each temperature considered. This permitted determination of the goodness of the fit between the measured and model predicted HSP expression values. A perfect fit is denoted as a value of one and the accuracy of the fit declines as the correlation coefficient becomes smaller. The correlation coefficient between the measured and model predicted Hsp27 and Hsp70 expressions for PC3 and RWPE-1 cells for all temperatures was greater than 0.9, confirming the accuracy of the model for HSP prediction.

Cell viability

Figure 7 (adapted from [63]) shows histograms for control, methanol treated, severely heat shocked (complete cell death), and a typical heated sample, with the marker M1 denoting the dead cell population. The events label on the y-axis corresponds to cell number. The cell viability values for PC3 cells at 72 h PH are shown in Figure 8A (adapted from [63]). With increasing thermal stimulation temperature, injury increases uniformly and more rapidly. The highest measured temperature, 60°C, yielded less than 1% live cells for the shortest heating duration of 1 min; whereas the lowest temperature of 44°C with the longest duration of 30 min maintained a cell viability of 10%. The standard deviation in the cell viability measurement was in the range of 0.4–6.5% with the average standard deviation of ±3.5%.

The corresponding data for RWPE-1 cells are shown in Figure 8B (adapted from [63]). The standard deviation for the cell viability measurement was in the range of 0.4–6.3%, with the average standard deviation ±2.9%. The higher viabilities for identical temperature histories showed that the RWPE-1 cells were slightly less sensitive to thermal stress. However, the largest difference between the PC3 and RWPE-1 cell viabilities was in the range of 1–13%, with the largest variation in cell viabilities only twice the largest standard deviation value.

Correlation of HSP expression with cell viability

Understanding and predicting the relationship between HSP expression and cell viability is

important when designing adequate hyperthermia protocols. The HSP expression and cell viability data for PC3 cells are plotted together in Figures 9A–B (for Hsp70) and 9C–D (for Hsp27) to facilitate direct comparison as a function of stress temperature and time. Decreases in cell viability were observed for conditions less stressful than those required to achieve the largest increase in HSP expression. The cells demonstrated a greater sensitivity to injury than to an increment in HSP expression elevation with higher stress temperatures. At temperatures above 52°C, the level of HSP expression remained below the preheating value, and the cell viability plummeted precipitously. The responses at 58° and 60°C were indistinguishable and were presented as a single plot for T = 58°C. Data were not shown for Hsp60 because the absolute magnitude of expression elevation in response to thermal stress is minimal.

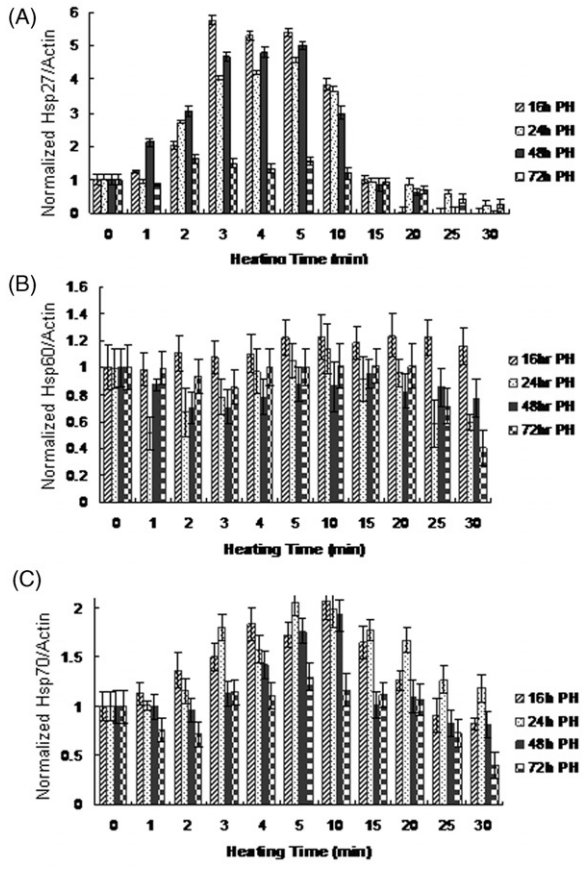

Figure 5. Normalised (A) Hsp27/actin, (B) Hsp60/actin, and (C) Hsp70/actin levels for PC3 cells as a function of heating time at $T = 44$°C and evaluation at various post-heating (PH) periods with an average standard deviation in HSP expression measurement of $\pm 0.12\,\mathrm{mg\,mL^{-1}}$, $n = 3$.

Arrhenius injury model

The cell viability data was employed to calculate the Arrhenius injury parameters to characterise the cells' injury response to hyperthermia. At each temperature the threshold time (τ) was determined for $\Omega = 1$ for which $C_\tau = 1/\mathrm{e}$ of C_o. For isothermal stress conditions, when $\Omega = 1$ the cell injury, Equation 4 simplifies to the logarithmic form:

$$\ln(\tau) = \left[(E_a/R) \cdot \frac{1}{T}\right] - \ln(A) \qquad (5)$$

Figures 10A and 10B present the relationship between $\ln(\tau)$ and 1/T for PC3 and RWPE-1 cells. The thermal injury kinetic coefficients of A and E_a were determined from the intercept and slope, respectively, of the best-fit linear function for the experimental data. It is evident from the plots of $\ln(\tau)$ and $1/T$ for both cell types that there exists a discontinuity in the data, requiring two linear functions to be used with a breakpoint at 54°C. The experimental parameters for $T = 44° - 54$°C and $T = 56° - 60$°C were fitted more accurately by independent functions having dissimilar slopes.

Table I. Hsp27 and Hsp70 expression model parameters for PC3 and RWPE-1 cells calculated by $H(t, T) = Ae^{(\alpha(T)t - \beta(T)t^{\gamma(T)})}$ where $H(t, T)$ represents Hsp27 and Hsp70 expression normalised with respect to actin concentration.

	PC3 cells						RWPE-1 cells					
	HSP27 parameters			HSP70 parameters			HSP27 parameters			HSP70 parameters		
Temperature (°C)	α	β	γ	α	β	γ	α	β	γ	A	β	γ
44	0.91	0.23	1.54	2.43	2.2	1.03	0.1	0.01	1.98	0.18	0.06	1.34
46	6.89	5.83	1.07	0.38	0.12	1.39	0.23	0.07	1.43	0.09	0	2.55
48	64.48	62.75	1.02	9.39	8.72	1.04	20.29	19.68	1.01	1.16	0.77	1.19
50	10.64	8.46	1.32	174.15	173.32	1.01	66.92	66.04	1.01	20.47	19.91	1.01
52	−1.91	0.29	2.76	12.36	12.32	1.01	0.71	0.51	1.41	0.32	0.08	2.12
54	−4.56	12.64	0.94	−0.09	0	10.6	−0.2	3.36	11.61	0.19	0.02	3.25
56	23.18	23.41	1.01	23.18	23.41	1.01	1.36	2.74	2.34	18.89	20.4	1.24
58	0.99	22.01	1	−0.49	0.06	4.15	1	22.01	1	−0.17	2.59	2.15
60	0.99	22.01	1	−7.77	−4.39	1.1	1	22.01	1	0.61	3.4	1.69

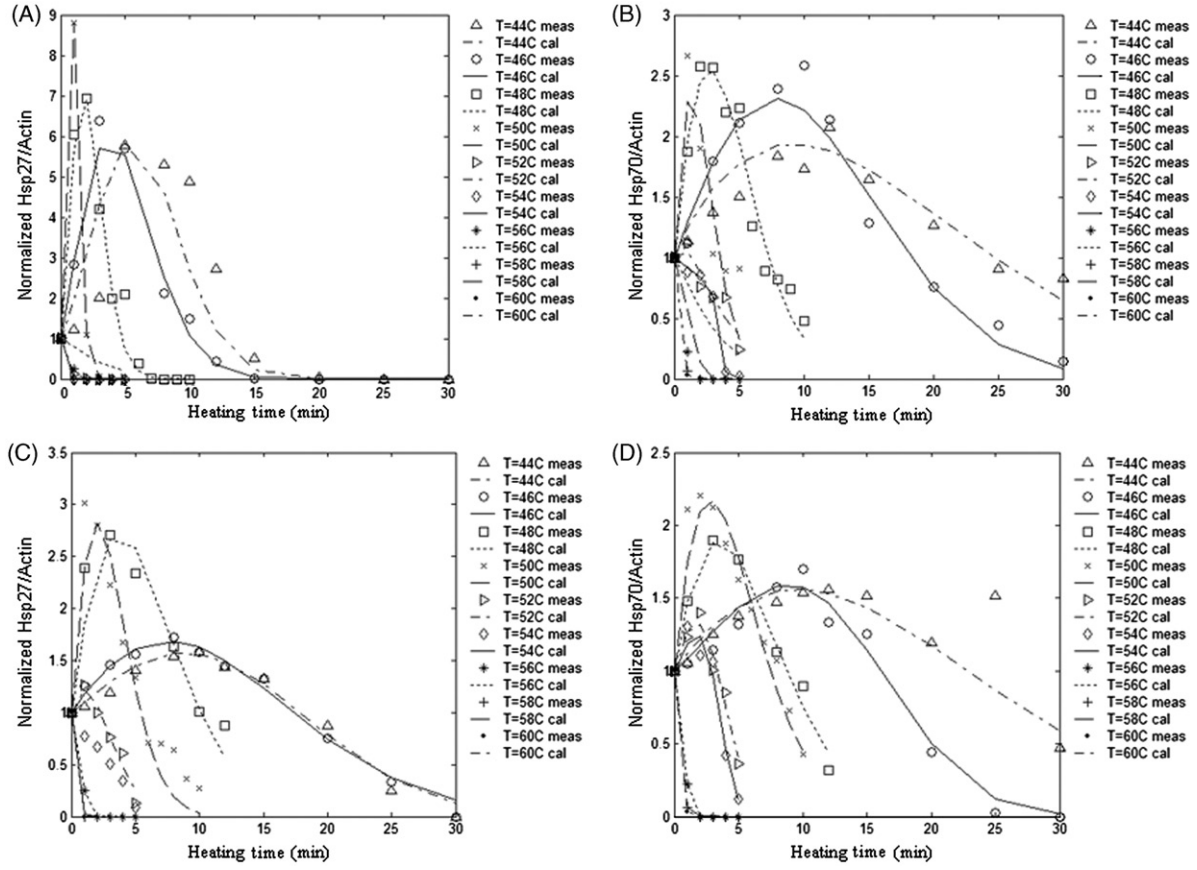

Figure 6. Comparison between measured and model-predicted (A) Hsp27 expression and (B) Hsp70 expression for PC3 cells and (C) Hsp27 expression and (D) Hsp70 expression for RWPE-1 cells.

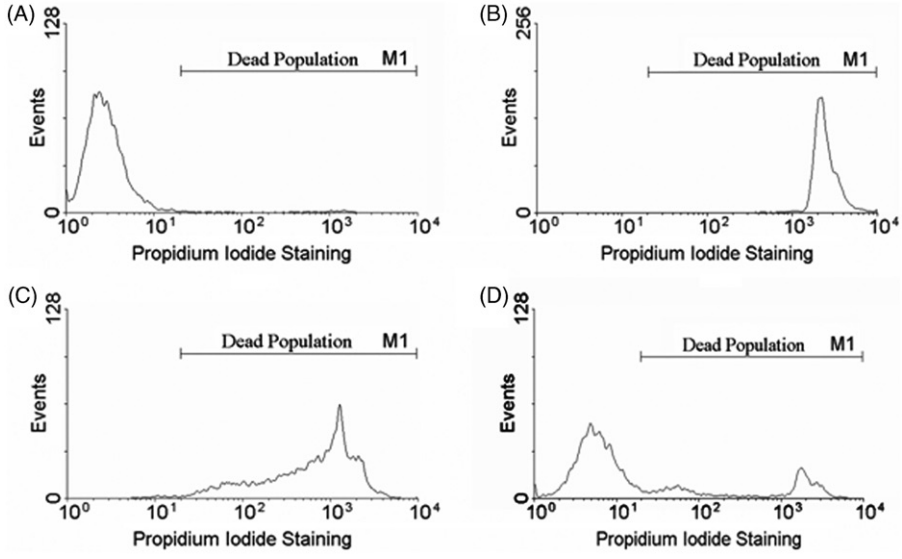

Figure 7. Flow cytometric analysis of cell viability (adapted from Feng et al. [63]). The dead cell population was defined by the marker (M1) as the region of the histogram occupied by both the methanol-treated and severely heat shocked samples (this region excluded the live population defined by the control sample). Cell viability determination is shown for (A) control (unheated), (B) methanol treated, (C) severely heat-shocked (52°C, 6 min), and (D) typical heated sample (44°C, 15 min).

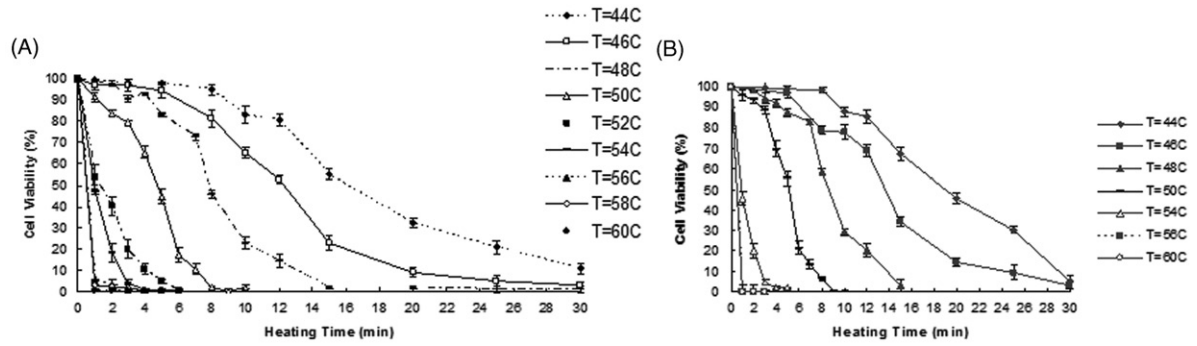

Figure 8. (A) PC3 cell viability in response to variable thermal stress duration as measured at 72 h PH with the average standard deviation in cell viability measurement of $\pm 3.5\%$, $n = 3$, (B) RWPE-1 cell viability in response to variable thermal stress duration as measured at 72 h post heating with the average standard deviation in cell viability measurement of $\pm 2.9\%$, $n = 3$.

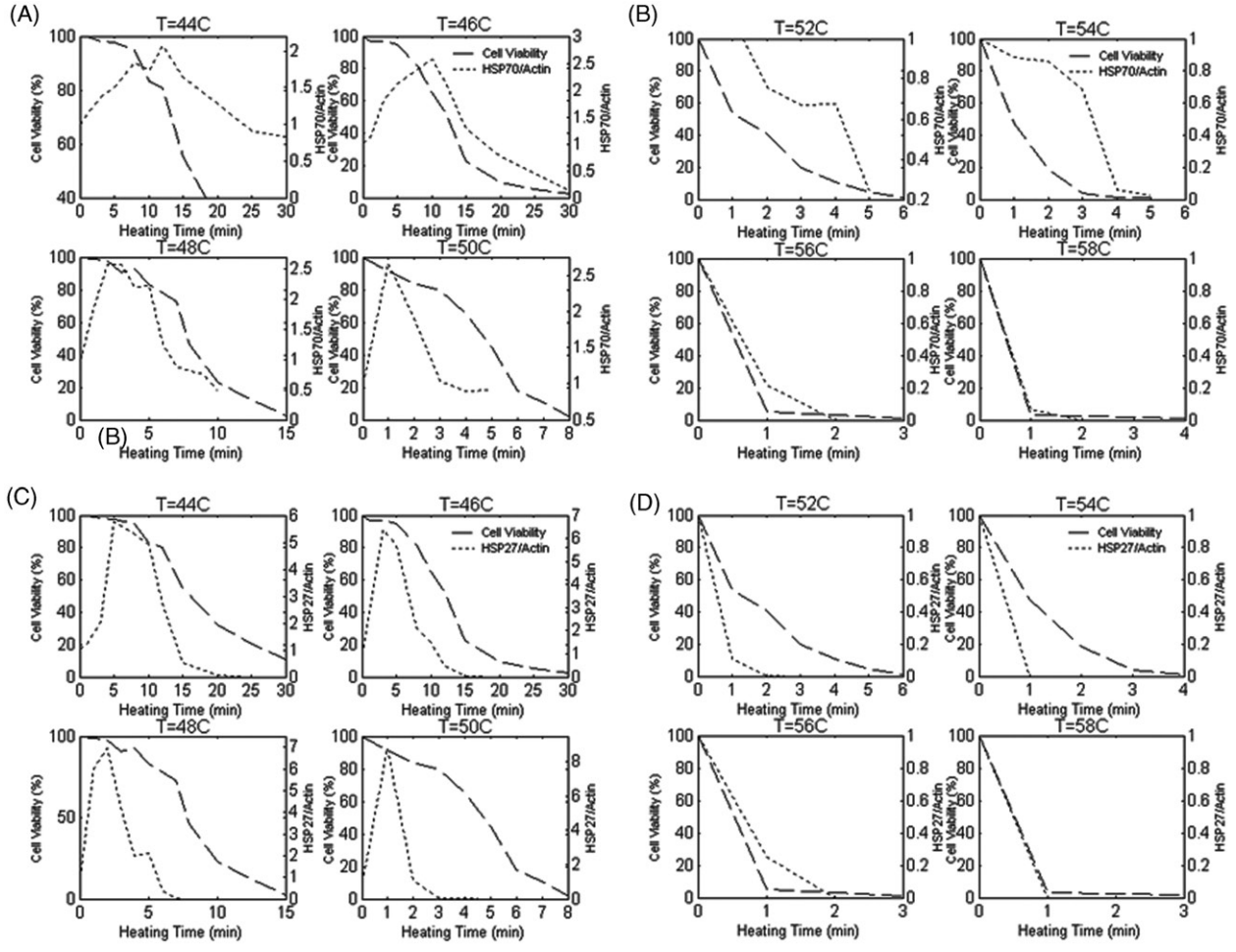

Figure 9. Comparison of measured cell viability with (A, B) Hsp70 and (C, D) Hsp27 in PC3 cells as a function of temperature and heating duration.

Thus, separate E_a and A values were determined for the two regimes of thermal injury for both cell types.

Table II presents the Arrhenius injury model constitutive parameter values for PC3 and RWPE-1 cells for the two thermal regimes of $T = 44^\circ - 54^\circ$C and $T = 56^\circ - 60^\circ$C. The values of E_a in the $T = 44^\circ - 54^\circ$C are nearly identical for both cell types; however, the A values are considerably larger for the RWPE-1 cells. In the $T = 56^\circ - 60^\circ$C regime the E_a and A values for the PC3 cells are 2.1 and 1.2×10^{10} times larger than the RWPE-1 values, respectively.

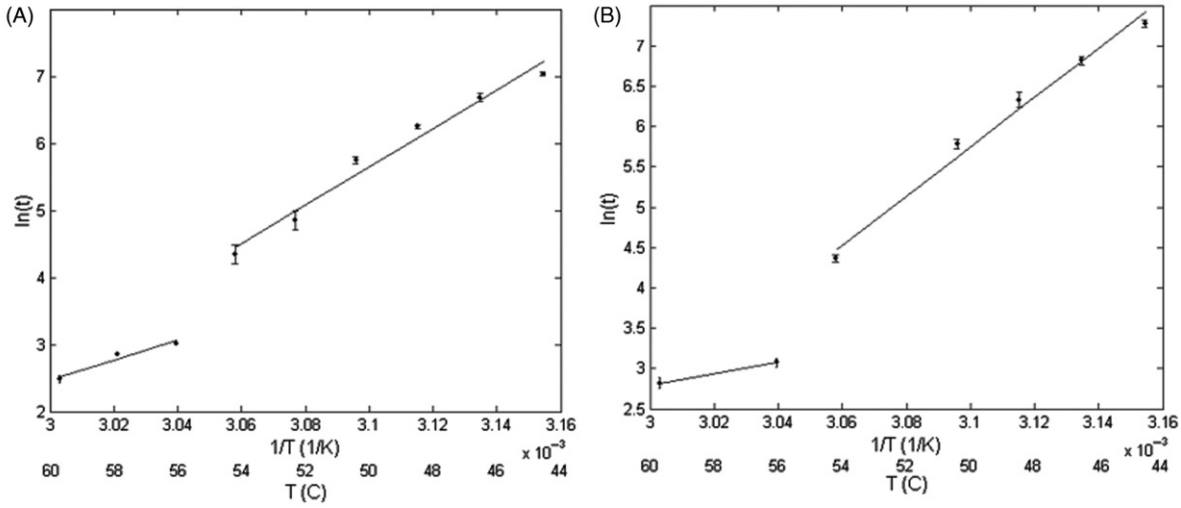

Figure 10. Natural logarithm of time as a function of $1/T$ for $\Omega = 1$ for (A) PC3 and (B) RWPE-1 cells.

Table II. Values of activation energy, E_a, and frequency factor A, for cell injury calculated by fitting the Arrhenius damage model to measured cell viability data for both cell types.

Cell type	E_a (J/mole) $T \leq 54^\circ C$	A (s^{-1}) $T \leq 54^\circ C$	E_a (J/mole) $T > 54^\circ C$	A (s^{-1}) $T > 54^\circ C$
PC3	2.38×10^5	1.8×10^{36}	1.24×10^5	7.0×10^{17}
RWPE-1	2.49×10^5	1.03×10^{38}	5.88×10^4	5.65×10^7

Injury model verification

To illustrate the accuracy of the model, the determined injury parameters, A and E_a, were employed to calculate the injury for all hyperthermia protocols. The calculated injury was then compared to the measured cell injury values, as shown in Figures 11A and 11B. The correlation coefficients between the model-predicted injury and measured injury data for both cell types and all temperatures were greater than 0.9, confirming the validity of the model.

Discussion

HSP expression

Significant Hsp27 and Hsp70 expression was induced following thermal stress, whereas Hsp60 elevation was minimal. The most dramatic increase in expression was associated with Hsp27, indicating that it may play a major role in protection following thermal stress in prostate cells. Enhanced Hsp70 expression was associated with a more dramatic decline in cell viability, requiring longer exposure periods at a given temperature. Despite the lower levels of Hsp70 expression, its persistence exceeded that of Hsp27. Hsp60 elevation in response to thermal stress was minimal, and therefore was considered an insignificant contributor to tumour protection induced by thermal therapy.

HSP expression in PC3 cells

Higher basal and thermally induced levels of Hsp70 and Hsp27 expression was induced in the PC3 cells. Following hyperthermia, Hsp70 expression was concentrated in the periphery of the cytoplasm, whereas Hsp27 expression was observed in more interior regions of the cytoplasm for PC3 cells. This localisation of Hsp70 to the periphery of the cytoplasm corresponds with studies conducted by Mambula et al.; however, they also observed the accumulation of Hsp70 in the nucleus of both PC3 and androgen-sensitive human prostate adenocarcinoma (LNCaP) cells [65]. A difference in heating protocols may contribute to the observation of Hsp70 accumulation in the nucleus. An additional study suggests that HSPs re-locate in response to hyperthermia; specifically, Hsp70 and Hsp27 move from the cytoplasm to the nucleolus and nucleus of fibrosarcoma (WEHI-S) cells [66]. Localisation of Hsp70 is thought to play a major role in contributing to cell proliferation; therefore targeting this accumulation may aid in enhanced cell necrosis [67].

The maximum expression levels for Hsp70 and Hsp27 were observed at a hyperthermia protocol of 1 min at 50°C, and the measured values were 2.7 times and 8.8 times the control, respectively. Longer durations at this temperature caused significant cell injury, leading to a decline in HSP expression. Temperatures greater than 50°C induced dramatic cell injury and protein denaturation. At lower temperatures, the rates and magnitudes of all HSP expression diminished proportionally.

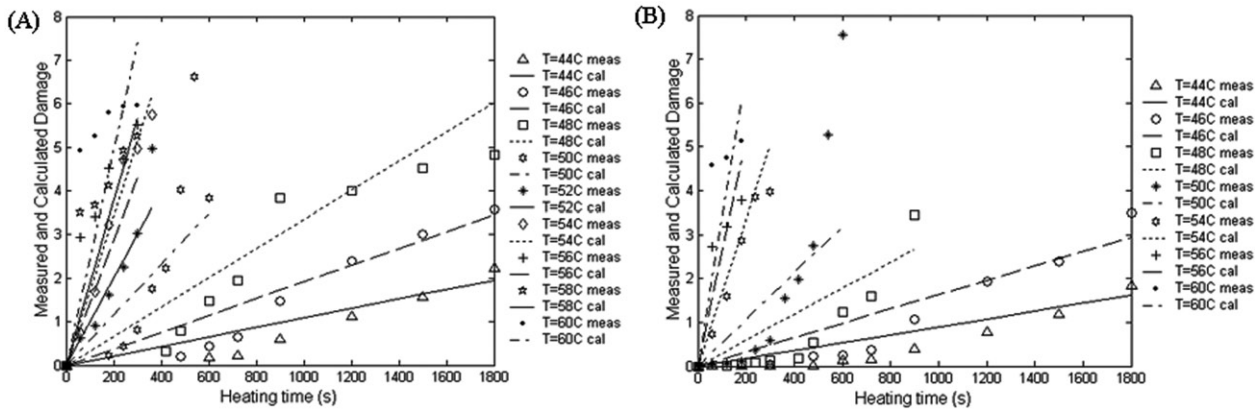

Figure 11. Comparison between measured and Arrhenius model-predicted damage for (A) PC3 and (B) RWPE-1 cells.

Although our study focused on higher heating temperatures (44°−60°C) than prior studies, our results correspond closely to previous studies where Hsp70 expression was elevated in PC3 cell monolayer following mild heat shock (43°C) [68, 69]. Very few papers exist that investigate thermally induced Hsp27 or Hsp60 expression in PC3 cells. However, a study performed with breast cancer cells showed that mild hyperthermia (42°C) will induce Hsp27 and Hsp70 levels 6-fold and 30-fold, respectively [70]. Variations in expression levels between the studies may be a result of heating technique (incubator versus water bath), heating temperature (mild versus severe hyperthermia), cell type (PC3 versus MDA MB231), and measurement technique (ELISA versus western blot).

If hyperthermia protocols that elicit HSP elevation are implemented in conjunction with subsequent thermal, radiation, or chemotherapy, knowledge of the duration of HSP expression up-regulation is critical to determining whether thermally induced cellular protection will diminish the benefit of combinatorial therapies. Therefore, the duration of Hsp27, Hsp60, and Hsp70 expression was measured for varying PH intervals. The peak expression level for all HSPs heated at 44°C occurred at approximately 16–24 h PH for PC3 cells. Following 48 h PH, all HSP expression began to diminish, and by 72 h, HSP expression was at the basal level. The implication is that any subsequent treatments implemented before 72 h may be compromised due to the residual elevations of Hsp27 and Hsp70. Previous studies by Wang et al. have measured the endogenous Hsp70 kinetics for bovine aortic endothelial cells following heating with an incubator at 42°C for 30 min to 5 h and recovery for 0 to 48 h at 37°C. This study also demonstrated sustained Hsp70 expression elevation for up to 48 h with Hsp70 concentration eight times greater than the basal level at 24 h post-heating [71].

Future studies will be necessary to determine the impact of varying amounts of HSP expression on the level of protection and enhanced tumour survival afforded against subsequent therapies, such as chemotherapy, radiation, or repeated thermal treatments, before predictions can be made regarding the tumour response. Based on determining the relationship between threshold levels of HSP expression and tumour recurrence, new dosimetry guidelines and computational models for predicting patient prognosis to hyperthermia therapies could be developed.

HSP expression in RWPE-1 cells

The localisation of Hsp27 and Hsp70 expression within the RWPE-1 cells was variable, with Hsp70 expression accumulation in the periphery of some cells and in the nucleus of other cells. The observed Hsp70 localisation corresponds with previous studies conducted by Mambula et al. for their LNCaP control cells which were exposed to two different heat treatments (43°C for 30 min and 40°C for 6 h) [65]. Exposure to hyperthermia conditions elicited much lower Hsp27 and Hsp70 expression and higher Hsp60 elevation in RWPE-1 cells compared to the PC3 cells. Maximum expression levels of 3.8, 1.5, and 2.3 times the control occurred for Hsp27, Hsp60, and Hsp70, respectively, at 50°C for 3 min. The lower sensitivity of the RWPE-1 cells to hyperthermia enabled them to prolong the HSP expression process longer than the PC3 cells, which demonstrated a decline in HSP expression and cell viability after only 1 min of heating at 50°C. Due to the lower HSP expression in the normal prostate cells, the corresponding thermo-tolerance associated with hyperthermia would be expected to be lower.

HSP expression model

The thermally induced HSP kinetics data measured by western blotting facilitated the development of an

empirical mathematical model for prediction of HSP expression in PC3 and RWPE-1 cells due to a wide range of temperatures. Only Hsp27 and Hsp70 data were incorporated into the formulation of the model since induction of Hsp60 expression was insensitive to thermal stress. This is the first predictive model for thermally induced HSP expression. Utilisation of the mathematical formulation of the empirical model and the expression parameters permitted prediction of the HSP expression phenomena with high accuracy, providing insight into the expected tissue response due to hyperthermia.

Cell viability

The rate of cell viability decline is more rapid as the stress temperature is increased. PC3 cells exhibited a slightly greater sensitivity to thermal stress than the RWPE-1 cells, demonstrated by their lower cell viabilities following heating. A more drastic difference in cell viability between the PC3 and RWPE-1 cells was expected due to the sensitivity of prostate tumour tissue to hyperthermia treatment. Although our in vitro studies did not reflect significant differences in cell viability between the two cell types, previous studies have demonstrated a much lower thermal threshold for destruction of AT-1 and PC3 tumours in vivo compared to their in vitro counterparts under similar conditions [68, 72, 73]. Specifically, work conducted by Tang et al. suggests that while heat shock response of in vivo PC3 tumours is significantly less than the in vitro response, targeting Hsp70 may still aid in the success of subsequent thermal or chemotherapeutic treatments [68]. This differential response is most likely due to the presence of the vascular network in vivo, which is easily destroyed during thermal therapy leading to hypoxia, ischaemia, and accelerated tumour death [73, 74]. Thus, further investigation of the hyperthermia induced HSP expression kinetics and cell viability modifications for PC3 tumours in vivo will be essential before final dosimetry guidelines are developed for prostate cancer therapy.

Cell viability and HSP expression design protocols

The success of the combined thermal therapy and subsequent radiation or chemotherapy treatments rely on identifying and avoiding hyperthermia protocols that induce HSP expression elevation. This study has determined temperature–time combinations for typical hyperthermia therapies, where HSP expression is elevated and cell viability is high. Designing hyperthermia protocols that minimise both HSP expression and cell viability in the tumour will improve the effectiveness of subsequent therapies. Table III shows suggested hyperthermia protocols to reduce Hsp70 and Hsp27 expressions below the basal level, decreasing thermally induced tumour protection. The thermal stress conditions that cause Hsp70 expression to decline are more severe than necessary for Hsp27 degradation. As a result, the Hsp70 protocol guidelines define the most rigorous criteria for hyperthermia protocol design.

Table III. Minimum threshold heating protocols to diminish Hsp27 and Hsp70 expression below the basal level.

Temperature (°C)	Hsp70 heating duration (min)	Hsp27 heating duration (min)
44	25	15
46	20	12
48	7	6
50	4	3
52	2	1
54	1	1
56	1	1
58	1	1
60	1	1

Cell injury

Arrhenius injury parameters were determined to permit prediction of cell injury for a wider range of hyperthermia protocols than were measured. A breakpoint in the thermal injury rate process was identified at 54°C for both cell types, yielding distinct E_a and A values above and below this temperature. The breakpoint may occur as a consequence of different thermal injury mechanisms for temperatures above and below 54°C. Conversely, the breakpoint may result from non-isothermal heating due to the water bath time constant (longer than 1 min at temperatures greater than 52°C) for brief heating duration protocols (1–3 min) employed in determining injury parameters for $T > 54$°C. In a similar study, AT-1 cells were described as having an injury process breakpoint at 55°C, where it was hypothesised to be a consequence of a change in the mechanism of thermal injury [75]. In order to confirm the breakpoint as a legitimate phenomenon, sources with a shorter thermal equilibration constant should be employed, such as ultrasound, microwaves, radiofrequency, and lasers. The Arrhenius injury parameters determined for PC3 and RWPE-1 cells in this study compare well with the parameters presented for AT-1 cells in which injury was measured using calcein leakage and propidium iodide staining performed by Bhowmick et al. [72]. This group reported parameters of $81.33\,\mathrm{kJ\,mol^{-1}}$ and $5.069 \times 10^{10}\ \mathrm{s^{-1}}$ for E_a and A (calcein leakage), and $244.8\,\mathrm{kJ\,mol^{-1}}$ and $2.99 \times 10^{37}\,\mathrm{s^{-1}}$ for E_a and A (propidium iodide), respectively, for temperature ranges from 40 to 70°C [72].

Hyperthermia protocols were identified that produced Hsp27, Hsp60, and Hsp70 elevation in both normal and prostate cancer cells. The HSP expression kinetics data enabled development of the first thermally induced HSP expression predictive model. Injury model parameters were determined to predict cell injury at elevated temperatures. Utilisation of the HSP expression model and injury parameters determined in this study should facilitate the design of more effective treatment protocols for prostate cancer. The dosimetry guidelines developed will redefine the required thermal dose standards to permit minimal HSP induction following hyperthermia therapy. This HSP expression predictive model can be integrated into current treatment planning models to predict the thermally induced HSP expression and related tumour recurrence for potential hyperthermia therapies.

Declaration of interest This research was funded by the Abell-Hanger Foundation, the National Science Foundation Awards, CTS-0332052 and CNS-0540033, and the Robert and Prudie Leibrock Professorship in Engineering at the University of Texas at Austin, and was performed at the University of Texas at Austin.

References

1. What are the key statistics about prostate cancer? American Cancer Society 2009. Available from: http://www.cancer.org/docroot/CRI/content/CRI_2_4_1X_What_are_the_key_statistics_for_prostate_cancer_36.asp (updated 7 July 2009; cited 18 January 2010).
2. Stern JM, Stanfield J, Kabbani W, Hsieh JT, Cadeddu JA. Selective prostate cancer thermal ablation with laser activated gold nanoshells. J Urol 2008;179:748–753.
3. Mertyna P, Goldberg W, Yang W, Goldberg SN. Thermal ablation: A comparison of thermal dose required for radiofrequency-, microwave-, and laser-induced coagulation in an ex vivo bovine liver model. Acad Radiol 2009;16:1539–1548.
4. Yerushalmi A, Servadio C, Leib Z, Fishelovitz Y, Rokowsky E, Stein JA. Local hyperthermia for treatment of carcinoma of the prostate: A preliminary report. Prostate 1982;3:623–630.
5. Johannesen M, Gneveckow U, Thiesen B, Taymorrian K, Cho CH, Waldofner N, Scholz R, Jordan A, Loening SA, Wust P. Thermotherapy of prostate cancer using magnetic nanoparticles: Feasibility, imaging, and three-dimensional temperature distribution. Eur Urol 2007;52:1653–1662.
6. Horsman MR, Overgaard J. Hyperthermia: A potent enhancer of radiotherapy. Clin Oncol 2007;19:418–426.
7. van der Zee J, Gonzalez Gonzalez D, van Rhoon GC, van Dijk JDP, van Putten WLJ, Hart AAM. Comparison of radiotherapy alone with radiotherapy plus hyperthermia in locally advanced pelvic tumors: A prospective randomised multicentre trial. Lancet 2000;355:1119–1125.
8. Gilligan T, Kantoff PW. Chemotherapy for prostate cancer. Urology 2002;60:94–100.
9. Calabro F, Sternberg CN. Current indications for chemotherapy in prostate cancer patients. Eur Urol 2007;51:17–26.
10. Potters L, Fearn P, Kattan MW. External radiotherapy and permanent prostate brachytherapy in patients with localized prostate cancer. Brachytherapy 2002;1:36–41.
11. Monrow AT, Faricy PO, Jennings SB, Biggers RD, Gibbs GL, Peddeda AV. High-dose-rate brachytherapy for large prostate volumes (>50cc) – Uncompromised dosimetric coverage and acceptable toxicity. Brachytherapy. 2008;7:7–11.
12. Ponce AM, Vujaskovic Z, Yuan F, Needham D, Dewhirst MW. Hyperthermia mediated liposomal drug delivery. Int J Hyperthermia 2006;22:205–213.
13. Peer D, Karp JM, Hong S, Farokhzad OC, Margalit R, Langer R. Nanocarriers as an emerging platform for cancer therapy. Nat Nanotechnol 2007;2:751–760.
14. Bidwell III GL, Davis AN, Fokt I, Priebe W, Raucher D. A thermally targeted elastin-like polypeptide-doxorubicin conjugate overcomes drug resistance. Invest New Drugs 2007;25:313–326.
15. Oden JT, Diller KR, Bajaj C, Browne JC, Hazle J, Babuska I, Bass J, Demkowicz L, Feng Y, Feuentes D, Prudhomme S, Rylander MN, Stafford RJ, Zhang Y. Development of a computational paradigm for laser treatment of cancer. Lect Notes Comput Sci 2006;3993:530–537.
16. Madersabacher S, Grobl M, Kramer G, Dirnhoger S, Steiner G, Marberger M. Regulation of heat shock protein 27 expression of prostastic cells in response to heat treatment. Prostate 1998;37:174–181.
17. Rylander MN, Diller KR, Wang S, Aggarwal S. Correlation of HSP70 expression and cell viability following thermal stimulation of bovine aortic endothelial cells. J Biomech Eng 2005;127:751–757.
18. Rylander MN, Feng Y, Bass J, Diller KR. Coordinated modeling of thermal stress induced cell injury and heat shock protein expression. Ann N Y Acad Sci 2005;1066:222–242.
19. Wang S, Xie W, Rylander MN, Tucker PW, Aggarwal S, Diller KR. HSP70 kinetics study by continuous observation of HSP-GFP fusion protein expression on a perfusion heating stage. Biotechnol Bioeng 2007;99:146–154.
20. Vertrees RA, Jordan JM, Zwischenberger JB. Hyperthermia and chemotherapy: The science. In: Helm CW and Edwards RP, editors. Current Clinical Oncology: Intraperitoneal Cancer Therapy. Totowa: Humana Press; 2007. pp 71–100.
21. Vargus-Roig LM, Fanelli MA, Lopez LA, Gago FE, Tello O, Aznar JC, Ciocca DR. Heat shock proteins and cell proliferation in human breast cancer biopsy samples. Cancer Detect Prev 1997;21:441–451.
22. Cornford PA, Dodson AR, Parsons KF, Desmond AD, Woolfenden A, Fordham M, Neoptolemos JP, Ke Y, Foster CS. Heat shock protein expression independently predicts clinical outcome in prostate cancer. Cancer Res 2000;60:7099–7105.
23. Richards EH, Hickey E, Weber L, Masters JR. Effects of overexpression of small heat shock protein HSP27 on the heat and drug sensitivities of human testis tumor cells. Cancer Res 1996;56:2446–2451.
24. Ciocca DR, Clark GM, Tandon AK, Fuqua SAN, Welch WJ, Mc Guire WL. Heat shock protein HSP70 in patients with axillary lymph node-negative breast cancer: Prognostic implications. J Natl Cancer Inst 1993;85:570–574.
25. Fuqua SA, Oesterreich S, Hilsenbeck SG, Von Hoff DD, Eckardt J, Osborne CK. Heat shock proteins and drug resistance. Breast Cancer Res Treat 1994;32:67–71.
26. Landriscina M, Amoroso MR, Piscazzi A, Esposito F. Heat shock proteins, cell survival and drug

resistance: The mitochondrial chaperone TRAP1, a potential novel target for ovarian cancer therapy. Gynecol Oncol 2009.
27. Tomei LD, Cope FO. Apoptosis: The Molecular Basis of Cell Death. New York: Cold Spring Harbor; 1991.
28. Gibbons NB, Watson RWG, Coffey RNT, Brady HP, Fitzpatrick JM. Heat-shock proteins inhibit induction of prostate cancer cell apoptosis. Prostate 2000;45:58–65.
29. Creagh EM, Sheehan D, Cotter TG. Heat shock proteins – Modulators of apoptosis in tumour cells. Leukemia 2000; 14:1161–1173.
30. Garrido C, Solary E. A role of HSPs in apoptosis through 'protein triage'? Cell Death Differ 2003;10:619–620.
31. Takayama S, Reed JC, Homma S. Heat-shock proteins as regulators of apoptosis. Oncogene 2003;22:9041–9047.
32. Levine AJ, Momand J, Finlay CA. The p53 tumor supressor gene. Nature 1991;351:453–456.
33. Ciocca DR, Calderwood SK. Heat shock proteins in cancer: Diagnostic, prognostic, predictive, and treatment implications. Cell Stress Chaperones 2005;10:86–103.
34. Mehlen P, Kretz-Remy C, Preville X, Arigo AP. Human HSP27, Drosophillia HSP27, and human alpha B-crystallin expression-mediated increase in glutathione is essential for the protective activity of these proteins agaisnt TNF-alpha-induced cell death. EMBO J 1996;15:2695–2706.
35. Singh J, Kaur G. Hsp70 induction and oxidative stress protection mediated by a subtoxic dose of NMDA in the retinoic acid-differentiated C6 glioma cell line. Brain Res Bull 2006;69:37–47.
36. Oesterreich S, Weng CN, Qiu M, Hilsenbeck SG, Fuqua SAW. The small heat shock protein HSP27 is correlated with growth and drug resistance in human breast cancer cell lines. Cancer Res 1993;53:4442–4448.
37. Calderwood SK, Khaleque MA, Sawyer DB, Ciocca DR. Heat shock proteins in cancer: Chaperones of tumorigenesis. Trends Biochem Sci 2006;31:164–172.
38. Franzen B, Linder S, Alaiya AA, Erikson E, Fujioka K, Bergman AC, Jornvall H, Auer G. Analysis of polypeptide expression in benign and malignant human breast lesions. Electrophoresis 1997;18:582–587.
39. Van Buskirk AM, Enagel DC, Guagliardi LE. Cellular and sub-cellular distribution of HSP72/74: A peptide-binding protein that plays a role in antigen processing. J Immunol 1991;146:500–510.
40. Srivastava PK, Udono H, Blachere NE, Li Z. Heat shock proteins transfer peptides during antigen processing and CTL priming. Immunogenetics 1994;39:93–100.
41. Menoret A, Patry Y, Burg C, Pendu JL. Co-segregation of tumor immunogenicity with expression of inducible but not constitive Hsp70 in rat colon carcinomas. J Immunol 1995; 155:740–748.
42. Wei Y, Zhao X, Kariya Y, Fukata H, Teshigawara K, Uchida A. Induction of autologous tumor killing by heat treatment of fresh human tumor cell: Involvement of gd T cells and heat shock protein 70. Cancer Res 1996;56:1104–1113.
43. Udono H, Srivastava PK. Heat shock protein associated peptides elicit specific cancer immunity. J Exp Med 1986; 178:1391–1398.
44. Chant ID, Rose PE, Morris AG. Analysis of heat shock protein expression in myeloid leukemia cells by flow cytometry. Br J Haematol 1995;90:163–168.
45. Barnes JA, Dix DJ, Collins BW, Luft C, Allen JW. Expression of inducible Hsp70 enhances the proliferation of MCF-7 breast cancer cells and protects against the cytotoxic effects of hyperthermia. Cell Stress Chaperones 2001;6:316–325.
46. Beckham JT, Wilmink GJ, Mackanos MA, Takahashi K, Contag CH, Takahashi T, Jansen ED. Role of Hsp70 in cellular thermotolerance. Laser Surg Med 2008;40:704–715.
47. Georgopoulous C, Welch WJ. Role of the major heat shock proteins as molecular chaperones. Annu Rev Cell Biol 1993;9:601–634.
48. Craig EA, Weissman JS, Horwich AL. Heat shock proteins and molecular chaperones: Mediators of protein conformation and turnover in the cell. Cell 1994;78:365–372.
49. Kurahashi T, Miyake H, Hara I, Fujisawa M. Expression of major heat shock proteins in prostate cancer: Correlation with clinicopathological outcomes in patients undergoing radical prostatectomy. J Urol 2007;177:757–761.
50. Tiara T, Narita T, Iguchi-Ariga H. A novel G1-specific enhancer identified in the human heat shock protein 70 gene. Nucleic Acids Res 1997;25:1975–1983.
51. Daugaard M, Jaattela M, Rohde M. Hsp70-2 is required for tumor cell growth and survival. Cell Cycle 2005;4: 877–880.
52. O'Connel-Rodwell CE, Shriver D, Simanovskii DM, Mcclure C, Cao YA, Zhang W, Bachmann MH, Beckham JT, Jansen ED, Palanker D, Schwettman HA, Contag CH. A genetic reporter of thermal stress defines physiologic zones over a defined temperature range. FASEB J 2004;18:264–271.
53. Beckham JT, Mackanos MA, Crooke C, Takahashi T, O'Connel-Rodwell C, Contag CH, Jansen ED. Assessment of cellular response to thermal laser injury through bioluminescence imaging of heat shock protein 70. Photochem Photobiol 2004;79:76–85.
54. O'Connel-Rodwell CE, Mackanos MA, Simanovskii DM, Cao YA, Bachmann MH, Schwettman HA, Contag CH. In vivo analysis of heat-shock-protein-70 induction following pulsed laser irradiation in transgenic reporter mouse. J Biomed Opt 2008;13:030501.
55. Rieger TR, Morimoto RI, Hatzimanikatis V. Mathematical modeling of the eukaryotic heat-shock response: Dynamics of the Hsp70 promoter. Biophys J 2005;88:1646–1658.
56. Wang S, Aggarwal S, Diller KR. Heat shock protein 70 expression kinetics. J Biomech Eng 2003;125:794–797.
57. Burke A, Ding X, Singh R, Kraft RA, Rylander MN, Szot C, Buchanan C, Whitney J, Fisher J, Levi-Polyachenko N, Hatchr HC, D'Agostino Jr R, Nock N, Ajayan PM, Carroll DL, Torti FM, Torti SV. Rapid thermal treatment of kidney tumors with multi-walled carbon nanotubes results in long term survival. Proc Natl Acad Sci U.S.A. 2009;4: 12897–12902.
58. Fisher J, Rylander MN. Effective cancer laser therapy design through the integration of nanotechnology and computational treatment planning models. Proc SPIE 2008;68690D.1–68690D.11.
59. Jolly C, Morimoto RI. Role of the heat shock response and molecular chaperones in oncogenesis and cell death. J Natl Cancer Inst 2000;92:1564–1572.
60. Feige U, Mollenhauer J. Heat shock proteins. Introduction. Cell Mol Life Sci 1992;48:621–622.
61. Rylander MN, Feng Y, Zhang Y, Bass J, Stafford RJ, Volgin A, Hazle JD, Diller KR. Optimizing heat shock protein expression induced by prostate cancer laser therapy through predictive computational models. J Biomed Opt 2006; 11:041113.
62. Rylander MN, Feng Y, Bass J, Diller KR. Thermally induced injury and heat-shock protein expression in cells and tissues. Ann N Y Acad Sci 2005;1066:222–242.
63. Feng YS, Oden JT, Rylander MN. A two-state cell damage model under hyperthermic conditions: Theory and in vitro experiments. J Biomech Eng 2008;130:0410161–10.
64. Henriques FC. Studies of thermal injury, V. The predictability and the significance of thermally induced rate processes leading to irreversible epidermal injury. Arch Pathol 1947; 43:489–502.

65. Mambula SS, Calderwood SK. Heat shock protein 70 is secreted from tumor cells by a nonclassical pathway involving lysosomal endosomes. J Immunol 2006;177: 7849–7857.
66. Wissing D, Jaattela M. Hsp27 and Hsp70 increase the survival of WEHI-S cells exposed to hyperthermia. Int J Hyperthermia 1996;12:125–138.
67. Roti JLR, Kampinga HH, Malyapa RS, Wright WD, vanderWaal RP, Xu M. Nuclear matrix as a target for hyperthermic killing of cancer cells. Cell Stress Chaperones 1998;3:245–255.
68. Tang D, Khaleque MD, Jones EL, Theirault JR, Li C, Wong WH, Stevenson MA, Calderwood SK. Expression of heat shock proteins and heat shock protein messenger ribonucleic acid in human prostate carcinoma in vitro and in tumors in vivo. Cell Stress Chaperones 2005;10:46–58.
69. Moriyama-Gonda N, Igawa M, Shiina H, Urakami S, Shigeno K, Terashima M. Modulation of heat-induced cell death in PC-3 prostate cancer cells by the antioxidant inhibitor diethyldithiocarbamate. B J U Int 2002;90:317–325.
70. Ciocca DR, Fuqua SAW, Locklim S, Toft DO, Welch WJ, Mcguire WL. Response of human breast cancer cells to heat-shock and chemotherapeutic drugs. Cancer Res 1992;52:3648–3654.
71. Wang SH, Diller KR, Aggarwal SJ. Kinetics study of endogenous heat shock protein 70 expression. J Biomech Eng - Trans ASME 2003;125:794–797.
72. Bhowmick S, Swanlund DJ, Bischof JC. Supraphysiological thermal injury in Dunning AT-1 prostate tumor cells. J Biomech Eng - Trans ASME 2000;122:51–59.
73. Bhowmick S, Hoffman NE, Bischof JC. Thermal therapy of prostate tumor tissue in the dorsal skin flap chamber. Microvasc Res 2002;64:170–173.
74. Bhowmick SJ, Coad E, Swanlund DJ, Bischof JC. In vitro thermal therapy of AT-1 Dunning prostate tumours. Int J Hyperthermia 2004;20:73–92.
75. Bischof JC, Padanilam J, Holmes WH, Ezzell RM, Lee RC, Tompkins RG, Yarmush ML, Toner M. Dynamics of cell-membrane permeability changes at supraphysiological temperatures. Biophys J 1995;68:2608–2614.